Physica 23D (1986) 436–447
North-Holland, Amsterdam

LYAPUNOV ANALYSIS AND INFORMATION FLOW IN COUPLED MAP LATTICES

Kunihiko KANEKO
Institute of Physics, College of Arts and Sciences, University of Tokyo, Komaba, Meguro-ku, Tokyo 153, Japan and Center for Nonlinear Studies, Los Alamos National Laboratory, Los Alamos, NM 87545, USA*

Lyapunov analysis for the coupled map lattices is presented. The co-moving Lyapunov exponent is calculated, which is related with the propagation of the disturbance in space. The propagation speed agrees with the zero-crossing point of the co-moving Lyapunov exponent. The co-moving mutual information flow is introduced, which shows the selective transmission of the information at some speed. Lyapunov spectra and vectors are calculated. Spatial structures of the vectors are investigated. Possible analogy with the Anderson localization problem is discussed.

1. Introduction and models

Phenomena with spatio-temporal complexity are common in nature as are observed in the fluid, chemical, optical, and solid-state turbulence, pattern formation, neural networks, parallel computation problems and so on. Here, we use "coupled map lattices" as dynamical system models for the complexity.

A coupled map lattice is a dynamical system with a discrete time, discrete space, and continuous state [1–12]. Though there are various kinds of the above models, we restrict ourselves only to the following two cases here:

(I) *Diffusive coupling* [1–3]

$$x_{n+1}(i) = (1-\varepsilon)f(x_n(i)) + \varepsilon/2\{f(x_n(i+1)) + f(x_n(i-1))\},$$

(II) *One-way coupling* [1, 5, 6]

$$x_{n+1}(i) = (1-\varepsilon)f(x_n(i)) + \varepsilon f(x_n(i-1)),$$

where n is a discrete time step and i is a lattice point. The periodic boundary condition is adopted for model (I), while the boundary condition is fixed at $i=0$ (i.e., $x_n(0)=x^*$) for model (II). Here the mapping function $f(x)$ is chosen to be the logistic map ($f(x)=1-ax^2$) but the general features hold for a wide class of mappings such as the circle map ($x + A\sin(2\pi x) + D$).

Recent works have revealed the following aspects: For model (I) [2], (a) period-doubling of kink–antikink structures, (b) zigzag instability and transition from torus to chaos, (c) spatio-temporal intermittency and (d) the soliton turbulence; for model (II) [5, 6], (e) spatial amplification of noise and (f) flow of kink–antikinks.

Here we note that the spatial bifurcation can occur even if the dynamics itself is uniform in space. An example is a domain structure generated by the period-doubling in model (I) (see fig. 1). In the figure the motion is almost period-4 at

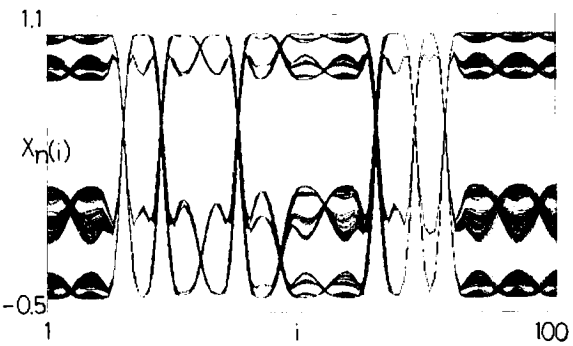

Fig. 1. Patterns for model (I) with $a = 1.42$ and $\varepsilon = 0.6$. $x_n(i)$'s are plotted superposedly for $n = 2000, 2001, \ldots, 3000$. $N = 100$. Random initial condition (RIC).

*Present and permanent address.

the region in a small domain, while it is almost period-8 at a larger domain, and so on. Thus, the state can differ by the lattice sites. Another example of the spatial bifurcation can be seen in the spatial period-doubling in open flow for model (II) [5].

In the present paper, we try to quantify the flow of disturbances and of the information in connection with the Lyapunov analysis.

2. Co-moving Lyapunov exponents

An important character in the spatially extended system is the growth of disturbance in "space-time". The growth of a small deviation in a chaotic system is usually quantified by the Lyapunov exponent. The conventional Lyapunov exponent itself, however, cannot characterize the propagation of a disturbance in space. Quite recently, Deissler and the author have introduced the "co-moving Lyapunov exponent" for the characterization [6].

The co-moving Lyapunov exponent is defined in the following way. First, we transform the frame from the stationary to a moving one. In the coupled map lattice system, this is performed by $i' = i - [vn]$ for the velocity v with i = lattice and n = time, where $[*]$ is the integer part of $*$. The co-moving Lyapunov exponent is calculated from the largest eigenvalue of the product of Jacobi matrices in the moving frame [6].

Let us explain the algorithm of the calculation and results in more detail for model (II).

We take a system with a large number of lattice points and choose a region $i_1 + [vn] < i < i_2 + [vn]$, where $i_2 - i_1$ is large enough for the average and v is the chosen velocity and n is the time step. We calculate the Jacobi matrix in that region for the moving frame and take a long time average of the product of the Jacobi matrices. The logarithm of the largest eigenvalue of the product divided by the time steps gives the co-moving Lyapunov exponent.

One important aspect of the open flow system is the convective instability [4, 6, 13]. In flow systems, some state can be unstable only in some moving frame. If model (II) is convectively unstable, the inclusion of a small noise is essential as was noted by Deissler [4, 13]. In the following, we consider model (II) with a homogeneously distributed noise $\sigma_n(i)$ added on every site and step.

2.1. *Stability of a homogeneous state*

First, we study the simplest case, i.e., the homogeneous state. Let us consider the evolution equation for the deviation $\delta x_n(i)$ from the fixed point solution $x(i) = x^*$, where x^* is a fixed point for the single logistic map (i.e., $x^* = \left(\sqrt{(1+4a)} - 1\right)/(2a)$). The equation is given by (see also [4])

$$\delta x_{n+1}(i) = (1-\varepsilon) f'(x^*) \delta x_n(i) + \varepsilon f'(x^*) \delta x_n(i-1). \tag{2.1}$$

The growth of a disturbance in the moving frame is obtained by the substitution of $i = vn$ into the solution of (2.1). The co-moving Lyapunov exponent for the state is given from the logarithm of the growth rate:

$$\lambda(v) = \lambda_0 + \log\{(1-\varepsilon)/(1-v)\} + \log\{(\varepsilon/v)/((1-\varepsilon)/(1-v))\}^v, \tag{2.2}$$

where $\lambda_0 = \log|f'(x^*)|$. The co-moving Lyapunov exponent for a spatially homogeneous and temporally periodic or chaotic state is obtained in the same way, and the result is represented simply by the substitution of the Lyapunov exponent for the one-dimensional map $x' = f(x)$ into λ_0 in (2.2).

Even if the conventional Lyapunov exponent is negative ($\lambda(0) < 0$), the maximum of the co-moving Lyapunov exponent ($\lambda(\varepsilon)$) can be positive, which shows that the homogeneous state is convectively unstable. If the co-moving Lyapunov exponent is positive at some velocity, the homogeneous state loses its stability. For an inhomoge-

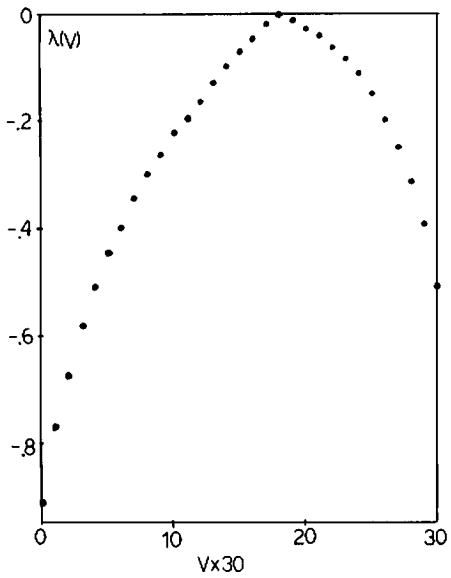

Fig. 2. The co-moving Lyapunov exponent $\lambda(v)$ as a function of v, for model (II) with $a = 1.5$ and $\varepsilon = 0.6$ and the noise strength σ is 10^{-5}. $i_1 = 1000$, $i_2 = 1100$, and calculation from the average through 15000 iterations after 1000 transients. $N = 16000$; $v = 0/30, 1/30, \ldots, 30/30$ (RIC).

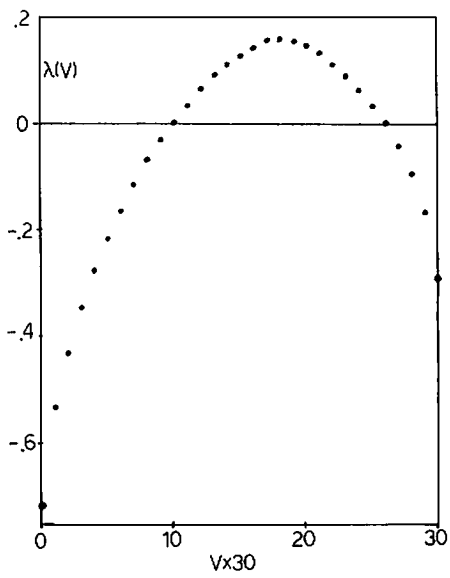

Fig. 3. The co-moving Lyapunov exponent $\lambda(v)$ as a function of v, for model (II) with $a = 1.6$ and $\varepsilon = 0.4$, and the noise strength σ is 10^{-8}. The same size, i_1, i_2, and numbers of iterations as for fig. 2. $v = 0/30, 1/30, \ldots, 30/30$ (RIC).

neous state we have to resort to the numerical calculation to obtain the exponent.

2.2. *Flow of kink–antikinks*

At the parameter region where the one-dimensional map $x' = f(x)$ shows the period-doubling bifurcation, model (II) shows the transmission of kink–antikinks to downflow [5]. An example of the calculation of the co-moving Lyapunov exponent is given in fig. 2. We note that the exponent has a maximum $\lambda(v) = 0$ at $v \approx \varepsilon$. This vanishing exponent corresponds to the "Goldstone mode" and the velocity $v \approx \varepsilon$ corresponds to the kink velocity.

2.3. *Turbulent case*

An example of the calculation of the co-moving Lyapunov exponent is shown in fig. 3, where the conventional exponent $\lambda(0)$ is negative even if the pattern and motion are chaotic. The exponent is positive only within the velocity band $v_1 < v < v_2$.

3. Propagation of disturbance and co-moving Lyapunov exponent

Let us perturb the lattice system $x_n(i)$ at one lattice site $i = i_0$ at the time step $n = m$. The perturbed system is denoted as $y_n(i)$. The motion of $y_n(i)$ obeys the same equation as $x_n(i)$ with

$$y_m(i) = x_m(i) \quad \text{for } i \neq i_0$$

and

$$y_m(i_0) = x_m(i_0) + \Delta,$$

where Δ represents the pulse input at $n = m$ and $i = i_0$. We plot the spatio-temporal region (n, i) where the difference between $y_n(i)$ and $x_n(i)$ exceeds some threshold δ. Examples of such patterns (which we call as difference patterns) are shown in

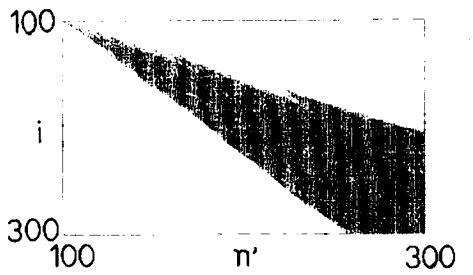

Fig. 4. The difference pattern for model (II) with the parameters corresponding to fig. 3. The dots are plotted on the region $|x_n(i) - y_n(i)| > 0.001$. The delta pulse with the strength $\Delta = 0.001$ is applied at the lattice site $i = 100$ at the time step 1000. The horizontal line is a time step $n' = n - 1000$ and the vertical line is a lattice space. $a = 1.5$ and $\varepsilon = 0.6$ and $\sigma = 10^{-5}$ (RIC).

fig. 4 for model (II) and in fig. 5a, b, c for model (I).

The velocity of the disturbance is defined as the speed of the propagation of the dotted region in the figures. The speed is essentially independent of the choice of the threshold value δ and is a well-defined quantity to characterize the spatio-temporal chaos.

3.1. *Open flow case (model II)*

The velocity obtained from these difference patterns can be calculated by the co-moving Lyapunov exponents. In the difference pattern in fig. 4, the existence of two velocities v_1 and v_2 is clearly seen. The corresponding co-moving Lyapunov exponent shown in fig. 3 crosses the zero value at the two velocities, which agree with the above two velocities v_1 and v_2. Since the co-moving Lyapunov exponent gives the growth rate at a given velocity, the propagation of disturbance is possible only in the region where $\lambda(v) > 0$. Thus, the propagation speed of the disturbance can be obtained from the velocity v which satisfies $\lambda(v) = 0$. This is a fundamental relation between the quantifiers in the spatio-temporal chaos.

3.2. *Diffusive coupling case (model I)*

There are three classes for the difference patterns for the chaotic motion in coupled map lattices. One is the localization of the disturbance (see fig. 5a). Even if the motion is chaotic, the chaos is confined (at least for a long time interval) in a domain separated by kinks which are gener-

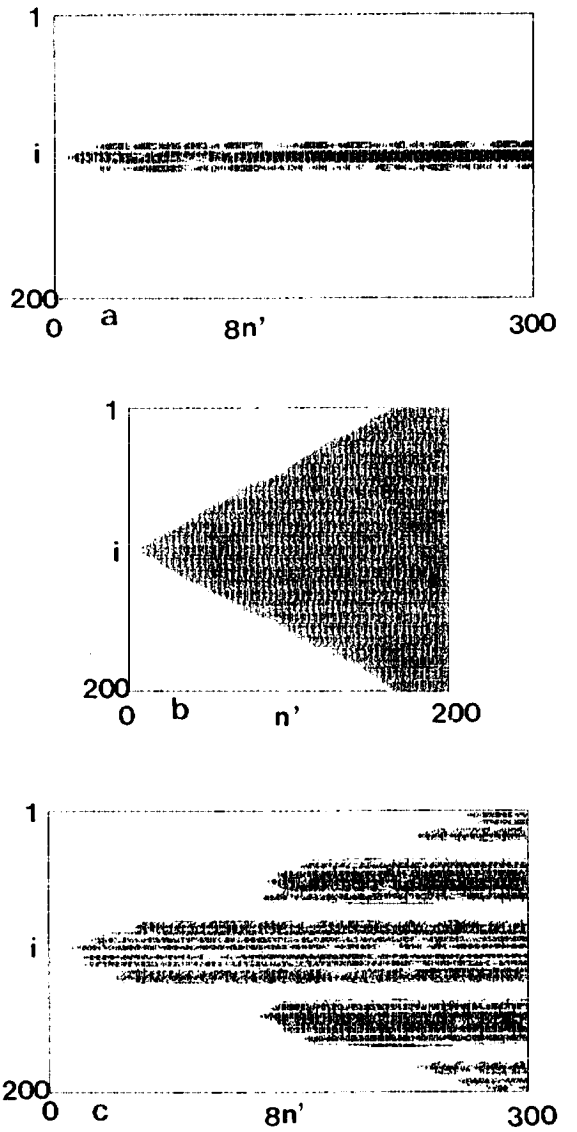

Fig. 5. The difference pattern for model (I). The dots are plotted on the region $|x_n(i) - y_n(i)| > 0.001$. The delta pulse with the strength $\Delta = 0.0001$ is applied at the lattice site $i = 100$ at the time step 500. The horizontal line is a time step $n' = n - 500$ and the vertical line is a lattice space. Initial condition is $x_0(i) = \cos(2\pi i/N)$ for (a) and (c), and random for (b). (a) $a = 1.405$ and $\varepsilon = 0.08$, localization (per 8 steps); (b) $a = 1.9$ and $\varepsilon = 0.6$, unbounded spreading; (c) $a = 1.41$ and $\varepsilon = 0.08$, tunneling (per 8 steps).

ated by period-doublings. Thus, the velocity of the propagation of disturbance is zero. This class of motion typically appears in the parameter region where the single logistic map shows the band-merging and at a small coupling. Another case is an unbounded spreading, in which the disturbed region spreads with almost a constant speed (of course with some fluctuations) (see fig. 5b). At the parameter region between these two classes of difference patterns, there appears a tunneling-like phenomenon (fig. 5c). The disturbance spreads till it reaches some kink positions where it stays a long time and then it starts to spread again to the next domain region. Thus, the propagation occurs in a stepwise manner.

If the disturbance propagates smoothly in space (i.e., the unbounded spreading), the propagation speed can be a well-defined quantity. The co-moving Lyapunov exponent is calculated in the same way as in the open flow case. An example is shown in fig. 6. The exponent is positive only in the region $v < v_1$. Again, the speed of the disturbance propagation in the difference pattern agrees with the above velocity v_1.

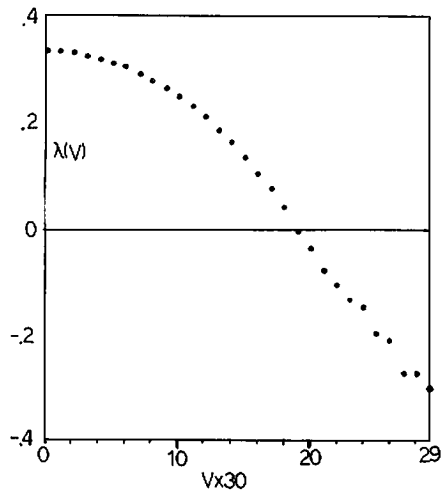

Fig. 6. The co-moving Lyapunov exponent $\lambda(v)$ as a function of v, for model (I) with the same parameters as in fig. 5b. $i_1 = 1$, $i_2 = 100$. Calculation from the average of 15000 iterations after 1000 transients. $N = 32000$; $v = 0/30$, $1/30, \ldots, 29/30$ (RIC).

4. Co-moving mutual information flow (COMIF)

One aspect of the chaotic system lies in the creation of information as was noted by Rob Shaw [14, 15]. In the spatially extended system, the information transmission is important. Here we study the information flow in space for model (II).

The mutual information between the two lattice points is calculated from the conditional probability. In order to study the flow of information, we define the mutual information between the values of x at two lattice points with a different time step. First, we calculate the conditional probability $P_{i\to j}(X, Y; v)\,\mathrm{d}X\,\mathrm{d}Y$ such that

$x_n(i)$ takes a value in $(X, X + \mathrm{d}X)$ and

$x_{n+[(j-i)/v]}(j)$ takes a value in $(Y, Y + \mathrm{d}Y)$.

Denoting the probability that $x(i)$ takes a value in $(x, x + \mathrm{d}x)$ by $p_i(x)\mathrm{d}x$, we define the mutual information flow from the lattice site i to the site j with the velocity v as

$$I(i \to j; v) = \int p_i(x) \log p_i(x)\,\mathrm{d}x + \int p_j(x) \log p_j(x)\,\mathrm{d}x - \iint P_{i\to j}(X, Y; v) \times \log P_{i\to j}(X, Y; v)\,\mathrm{d}X\,\mathrm{d}Y. \quad (4.1)$$

The quantity shows the coherence between the two sites at the different time given by the velocity v.

In fig. 7a, the COMIF is shown for various distances, where the parameter is chosen to be the case for the kink–antikink flow. We note the following features:

(i) COMIF has a sharp peak at $v \approx \varepsilon$, that is, at the velocity of kinks. The information is transmitted by kinks, which are generated by the noise. In other words, the information is created by the small noise as the phase switching of kink–anti-

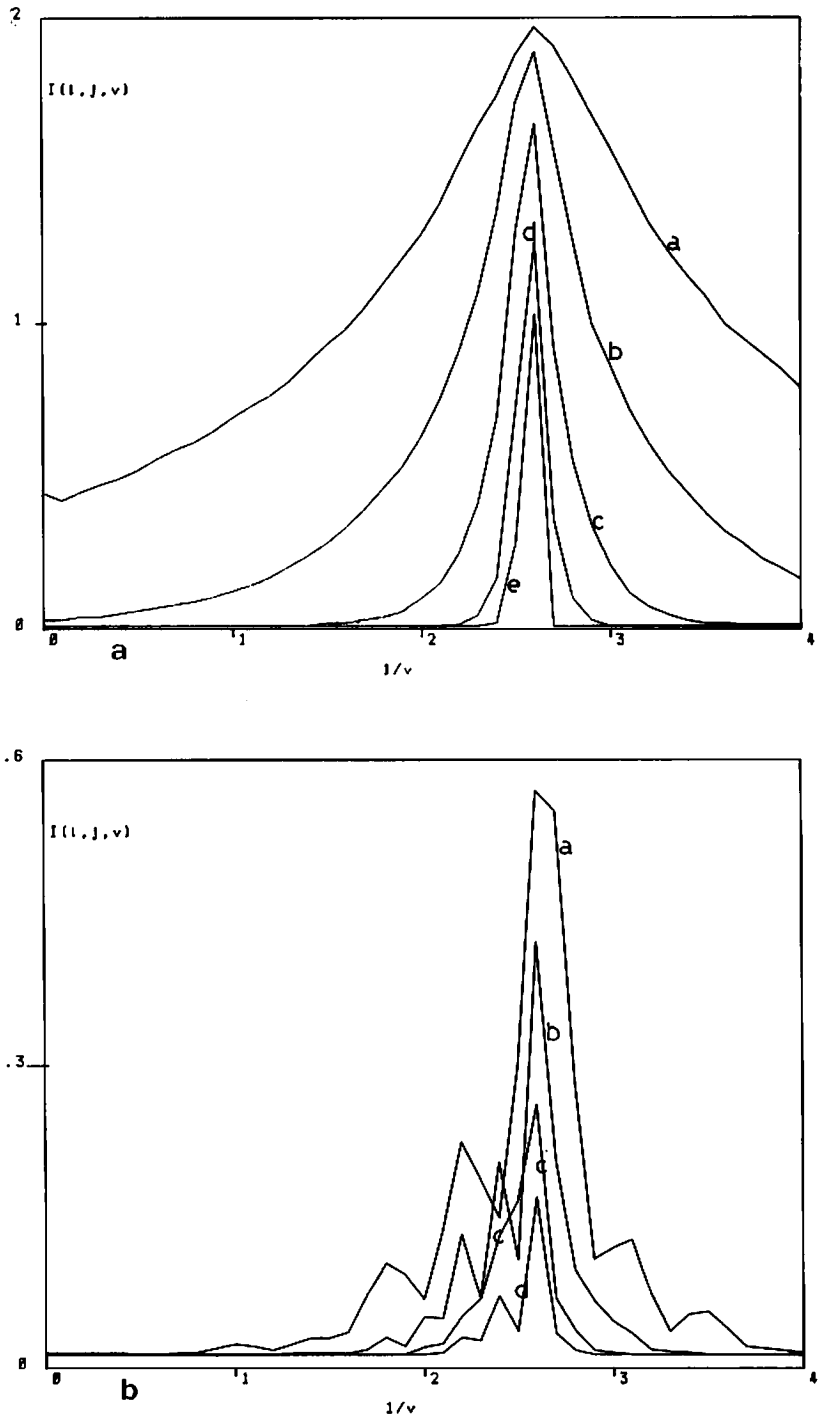

Fig. 7. Co-moving mutual information flow as a function of the inverse velocity $1/v$, for model (II) with (a) $a = 1.4$, $\varepsilon = 0.4$ and the noise strength $\sigma = 10^{-10}$ and (b) $a = 1.6$, $\varepsilon = 0.4$ and $\sigma = 10^{-10}$. The calculation of the probability P is performed by using 64 bins in the interval $(-1, 1)$ and through 100000 iterations. (a) $i = 140$; $j = 160$(a), 200(b), 320(c), 600(d), and 1000(e). (b) $i = 140$; $j = 160$(a), 180(b), 220(c), and 260(d).

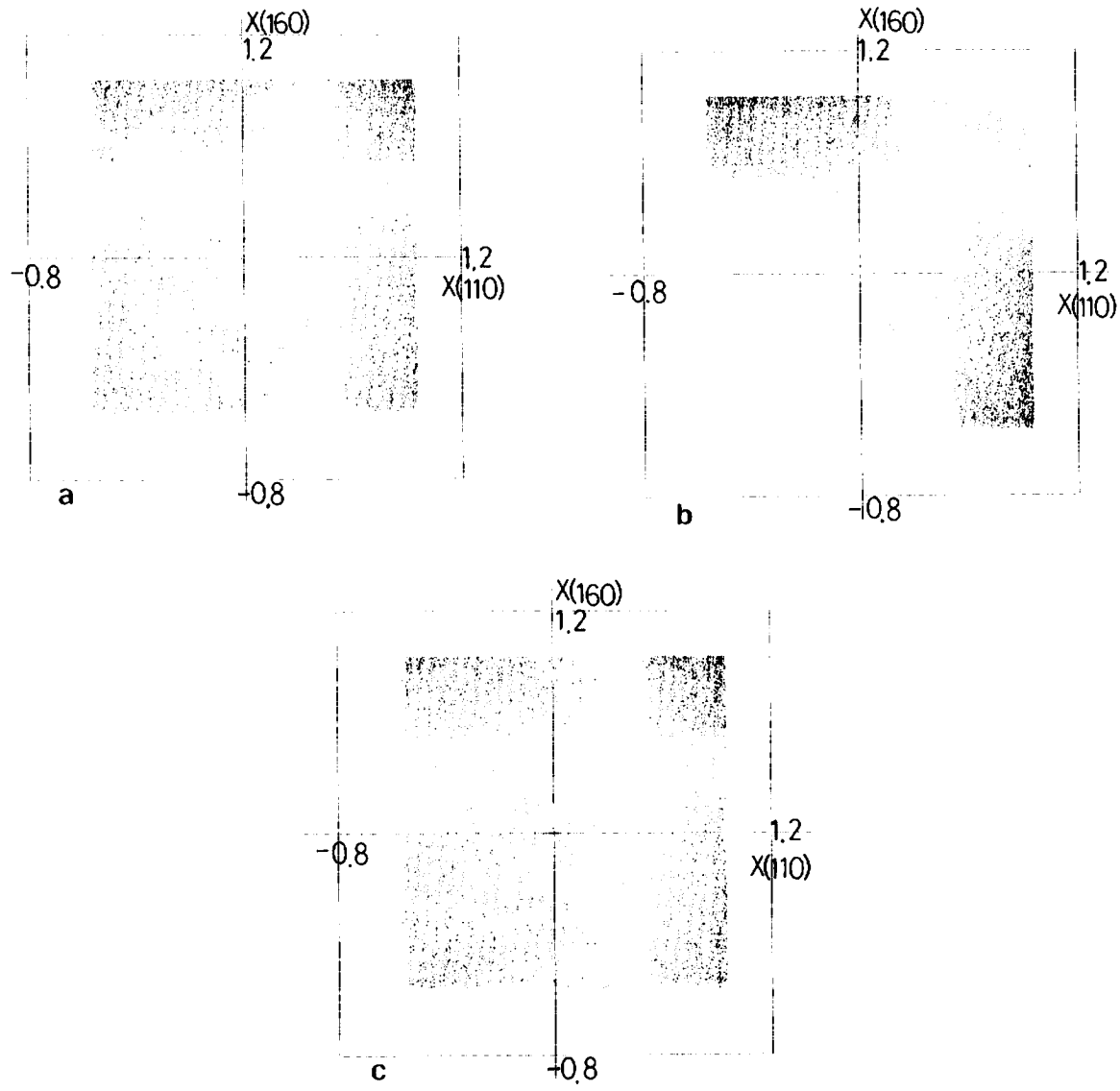

Fig. 8. Co-moving spatial Lorenz plot for model (II) with $a = 1.5$, $\epsilon = 0.6$, and $\sigma = 10^{-10}$. $(x_n(i), x_{n-[(j-i)/v]}(j))$'s are plotted for $i = 110$, $j = 160$ and $n = 5000, 5001, \ldots, 15000$ (RIC). (a) $v = 1/3$, (b) $v = 0.6$ and (c) $v = 1$.

kinks, which is transmitted through the kink motion.

(ii) The height of a peak decays exponentially with a rather slow rate, while the half-width of the peak decays exponentially with a much faster rate. Thus, the peak of COMIF is very sharp at distant points. This suggests that the coupled map lattice with period-doublings can be made use of as the information transmission line, since it has 2^k states for the information storage (k is the number of doublings) and it shows the selective propagation of information.

In fig. 7b the numerical result for the turbulent case is shown. In this case, we need not add the noise, since the information is created automatically by the chaotic motion. Again, the COMIF has a peak at the velocity $v \approx \epsilon$, at which the co-moving Lyapunov exponent has a maximum.

The peak, however, decays much faster. Especially, if the Lyapunov exponent is larger, it decays much faster.

To visualize clearly the selective flow of the information, we introduce the co-moving spatial Lorenz plot. The spatial Lorenz plot is the two-dimensional plot of $(x_n(i), x_n(j))$ for a fixed pair of (i, j) for a long time series. This plot is useful to detect the coherent motion in the turbulence, local oscillatory behaviors, and motion of kinks. The plot for a different time is powerful to detect the information flow. In fig. 8, sets of $(x_n(i), x_{n+[(j-i)/v]}(j))$ are plotted for various velocities. We note that the pattern is essentially a direct product of two independent chaotic motions for the velocities $v = 3.0^{-1}$ and 1.0, while it shows a remarkable correlation effect for the velocity $v \approx \varepsilon$.

5. Lyapunov analysis

In the present section, we investigate the Lyapunov spectra and vectors in the conventional sense, mainly focusing on the case of model (I). The coupled map lattice with the size N is an N-dimensional dynamical system. Through the long-time average of the product of Jacobi matrices, the N eigenvalues (Lyapunov exponents) and their eigenvectors (Lyapunov vectors) are calculated.

5.1. *Lyapunov spectra*

An example of the Lyapunov spectra is shown in fig. 9. If the expansion rate of the local dynamics is uniform (β), it can be shown that the spectra have the form of

$$\lambda_\kappa = \beta(1 + \varepsilon \cos(2\pi\kappa/N)). \tag{5.1}$$

If the expansion rate is not constant as is the case for a usual mapping (e.g., logistic or circle) and the spatial structure is inhomogeneous, there appears a deviation from the above form. For the initial few modes, the exponents roughly obey

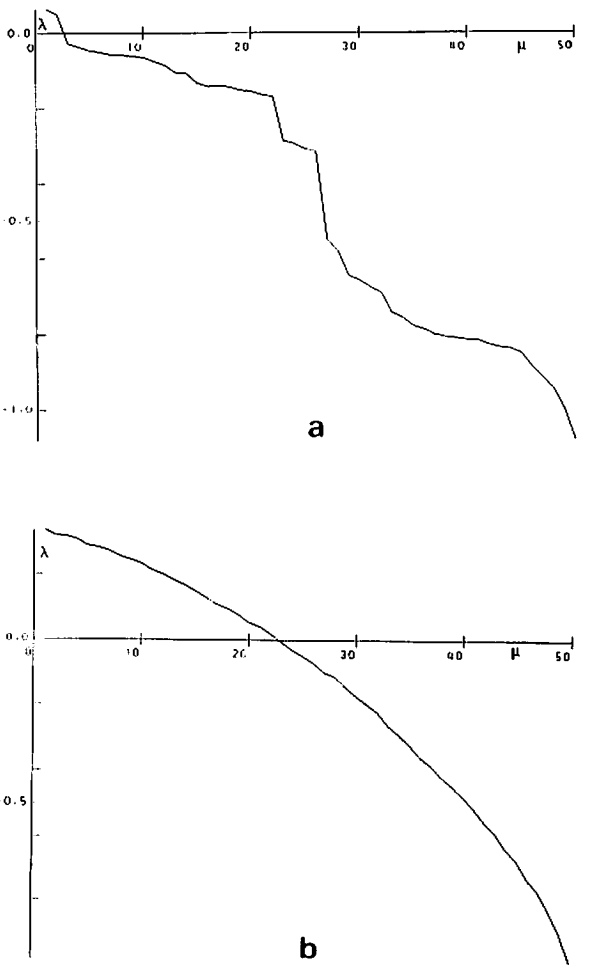

Fig. 9. Lyapunov spectra for model (I). The exponents are calculated from the average of 2500 steps after 1000 steps are discarded. $N = 50$. $x_0(i) = \sin(2\pi i/N)$. (a) $a = 1.5$ and $\varepsilon = 1/3$; (b) $a = 1.9$ and $\varepsilon = 1/3$.

$\lambda_\kappa \approx \lambda^0 - \alpha\kappa^2$. Near the onset of chaos, $\lambda^0 \propto a - a_c$, where a is the bifurcation parameter and a_c is the onset parameter for chaos. From the above arguments, the number of positive exponents and the Lyapunov dimension are expected to increase as $(a - a_c)^{1/2}$, which seems to roughly agree with the numerical result [1, 2].

Another aspect of the spectra is the stepwise strucure. If a kink separates the two neighboring domains, the system is essentially decomposed into the two subsystems. Then, the degeneracy of

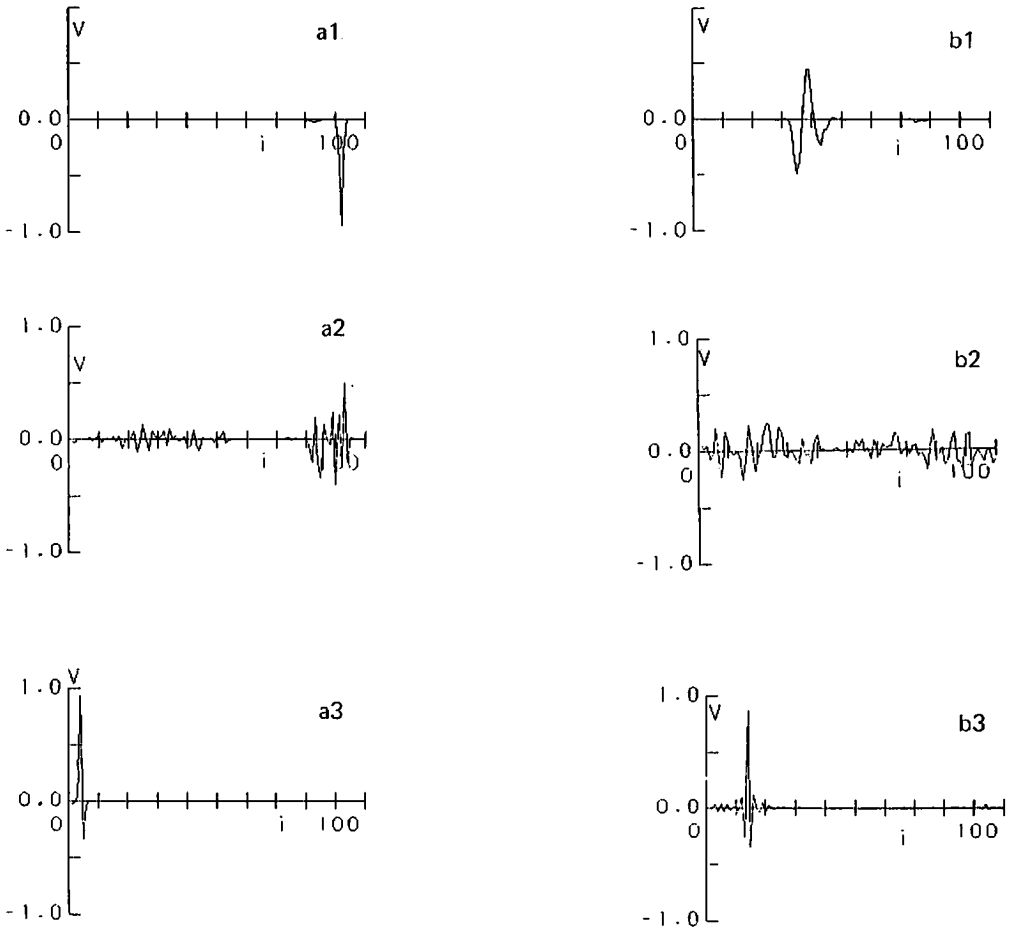

Fig. 10. Lyapunov vectors for model (I) after 2500 iterations of the successive Jacobi matrices. $x_0(i) = \sin(4\pi i/N)$.
(a) $a = 1.45$, $\varepsilon = 0.1$, and $N = 100$
(1) $v_1(i)$; the corresponding exponent = 0.106. The localized position is just at an antinode of a chaotic domain. (2) $v_{56}(i)$; the corresponding exponent = −0.14. (3) $v_{100}(i)$; the corresponding exponent = −0.57. The localized position is just at a kink.
(b) $a = 1.8$, $\varepsilon = 0.4$, and $N = 100$
(1) $v_1(i)$; the corresponding exponent = 0.304. (2) $v_{50}(i)$; the corresponding exponent = −0.127. (3) $v_{100}(i)$; the corresponding exponent = −0.162.

the spectra can occur. This is the origin of the stepwise strucure seen in fig. 9a. As the nonlinearity is increased, the band merging occurs, which brings about the successive merging of domains. The step strucure of the spectra, then, successively disappears (see fig. 9b).

5.2. *Lyapunov vectors*

Lyapunov vectors have more information on the spatio-temporal strucure than the spectra. Some vectors are localized in space, while some are extended for the whole space. The following features should be noted:

α) Weak-coupling case

If the coupling is small, Lyapunov vectors are localized in space. Some examples are shown in fig. 10a. Generally speaking, the vectors corresponding to the positive exponents are localized at the antinodes of domains, while the vectors for the large negative exponents are localized at the nodes (i.e., kinks).

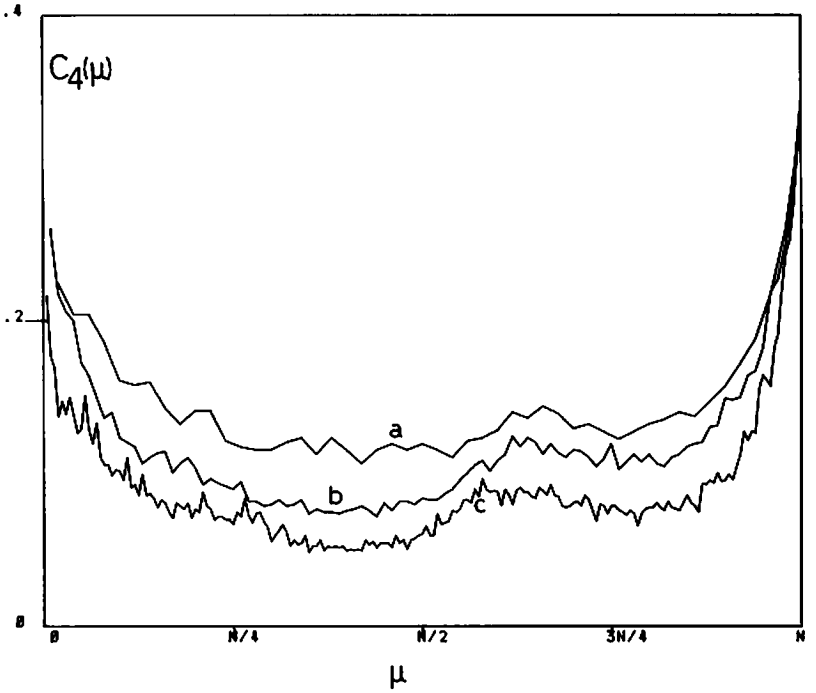

Fig. 11. The localization index $C_4(\mu)$ for model (I) with $a = 1.8$, $\varepsilon = 0.4$, and $N = 50$(a), $N = 100$(b), and $N = 200$(c). $x_0(i) = \sin(2\pi i/50)$.

β) Strong-coupling case

Some examples for the Lyapunov vectors are shown in fig. 10b. For the positive first few modes, the exponents are localized in space. As the exponent gets smaller, the corresponding vector includes higher wave numbers. The last few modes for the large negative exponents, again, are localized at the kink positions. This type of behavior can be commonly seen in the coupled map lattice system with a fairly strong coupling region ($0.3 \lesssim \varepsilon \lesssim 2/3$).

To characterize the localization of the Lyapunov vector, we introduce the following quantity:

$$C_4(\mu) = \sum_{i=1}^{N} v_\mu(i)^4, \tag{5.2}$$

where $v_\mu(i)$ is the Lyapunov vector corresponding to the μth exponent which satisfies the normalization condition $\sum_{i=1}^{N} v_\mu(i)^2 = 1$. If the mode is localized, the quantity $C_4(\mu)$ is $\mathcal{O}(1)$, while it is $\mathcal{O}(1/N)$ for the extended mode. An example of the behavior of the quantity is shown in fig. 11, which clearly shows the change "localization → extension → localization" as the mode number [16].

γ) Quantum mechanical analogy

The equation of the Lyapunov vector consists of the following two steps: (i) multiply the matrix $f'(x(i))\delta_{ij}$ to the vector $v_\mu(i)$ and (ii) multiply the matrix $(1-\varepsilon)\delta_{ij} + (\varepsilon/2)(\delta_{i,j+1} + \delta_{i,j-1})$ (the discrete diffusion operator), where δ_{ij} is the Kronecker delta. In the problem of the Schrödinger equation, we encounter with a similar problem. The diffusion operator corresponds to the $\partial^2/\partial x^2$ term, the $f'(x(i))$ term to the potential, Lyapunov spectra to the energy levels and the Lyapunov vectors to the eigen-wavefunctions. Of course, the correspondence is not so straightforward and it may be dangerous to pursue it too much. One possible conjecture, however, is the implication of Anderson localization [17]. In the

Schrödinger equation problem, the wavefunction is localized if the potential is random for one- and two-dimensional systems. In our problem, the term $f'(x(i))$ changes chaotically in space-time for the turbulent region and may have some relations with the two-dimensional system in a static random potential. This suggests that the similar mechanism with the Anderson localization makes the Lyapunov vector for the positive exponent localized. The numerical results seem to support this conjecture, though the detailed argument will be reported elsewhere.

δ) *Relation with the propagation of disturbances*

Let us recall the three patterns of the propagation of disturbance. First we expand the pulse input by the Lyapunov vectors. The important modes for the growth of a disturbance are the vectors for positive exponents. If a vector for a positive exponent localized at one domain does not have an overlapping with a vector at the neighboring domain, the disturbance cannot be propagated into the next domain. Thus, the localization of the disturbance in section 3 is explained by the nonoverlapping of the Lyapunov vectors for positive exponents. If the vectors at the neighboring domains have a very little overlapping, it takes a long time for the transmission of the disturbance by the overlapping term $\langle v_\mu | v_{\mu'} \rangle$. Thus, the propagation shows the tunneling-like phenomena as was shown in section 3. If the Lyapunov vectors for positive exponents at different domains have sufficient overlappings, the propagation shows the unbounded spreading.

6. Summary and discussion

In the present paper, spatial chaos is analyzed by the co-moving Lyapunov exponent, the propagation of disturbance, co-moving mutual information flow, and the Lyapunov spectra and vectors. Though these quantities are important for the characterization of spatio-temporal chaos, we have not yet fully understood their meaning and the relations among the quantities. Especially the following problems are important:

(i) Construction of the response theory of turbulent state based on the Lyapunov spectra and vectors.

(ii) In cellular automata problems, Wolfram and Packard [18] have used the term "Lyapunov exponents" in a different way from the conventional one, which essentially corresponds to the propagation speed in section 3. Thus, the co-moving Lyapunov exponent can give a relation with the two Lyapunov exponent terminologies in the dynamical system theory and in the cellular automata.

Another important aspect of turbulence is unpredictability. To predict the state after T time steps with the precision δ, we need the information about the present state with the precision $\delta \exp(-\lambda T)$, where λ is the maximum Lyapunov exponent. In the lattice system, the precision about the site j necessary for the prediction about the site i can differ by the distance $|j-i|$. For the prediction, we need the precision $\exp(-\lambda(|j-i|/T)T)$ about the present state at the site j, for the sites j's which satisfy $\lambda(|j-i|/T) > 0$, where $\lambda(v)$ is the co-moving Lyapunov exponent. This is another meaning for the co-moving Lyapunov exponent. It is important to construct the computation theory and to give some relations among the various quantities such as the spatio-temporal entropy and Lyapunov exponent.

(iii) The co-moving mutual information introduced in section 4 will be useful to analyze the information processing in spatio-temporal chaos. The quantity represents the degree of coherence of the phases of the oscillations at different sites. The sharp transmission of information by kinks may have some practical applications.

Coupled map lattices (CML) are new approaches towards the spatial chaos. One advantage in another familiar approach, cellular automaton (CA) is that it is closely connected with the computation theory, which may be summarized as the phrase "bit democracy" [19]. In CML, bits are used hierarchically and may not be so efficient as CA. The physical system (and the

present computer system), however, does not obey the bit democracy. The advantage in CML lies in the fact that we can understand the complex behavior in nature on the basis of the knowledge and methods of the (low-dimensional) dynamical system theory.

The connection of CML with the real physical system should be investigated in future. The open flow model (II) seems to have some features in common with the pipe flow experiment [20]. The algorithm to obtain the local dynamics and the coupling must be constructed in future as an extension of Takens' construction [21] to the spatio-temporal chaos.

Some extensions of CML will be of importance in the future. One is the coupled map network model with adaptive coupling, which will be useful as a simple model of neural networks, since the dynamics of a single neuron itself seems to be able to show a chaotic behavior.

Another model is a Hamiltonian version of CML. An example is a chain of the standard mapping with the coupling which satisfies the symplectic condition [22]. The model can show the spatial Arnold diffusion and may be a key model for the study of ergodicity.

Acknowledgements

I would like to thank Drs. D. Farmer, R. Deissler, J. Crutchfield, N. Packard, R. Shaw, G. Mayer-Kress, A. Bishop, and D. Campbell for useful discussions and their courtesy during my stay at Los Alamos. I am also grateful to the Institute of Plasma Physics at Nagoya for the facility of FACOM M-200 and VP-100.

References

[1] K. Kaneko, Ph.D. Thesis (1983) "Collapse of Tori and Genesis of Chaos in Dissipative Systems" (World Sci. Publ. Co., Singapore, 1986).
[2] K. Kaneko, Prog. Theor. Phys. 72 (1984) 480; 74 (1985) 1033.
[3] K. Kaneko, Physica 18D (1986) 475.
[4] R.J. Deissler, Phys. Lett. 100A (1984) 451.
[5] K. Kaneko, Phys. Lett. 111A (1985) 321.
[6] R.J. Deissler and K. Kaneko, preprint (1985) (LA-UR-85-3249) "Velocity-Dependent Lyapunov Exponents as a Measure of Chaos for Open Flow Systems".
[7] I. Waller and R. Kapral, Phys. Rev. 30A (1984) 2047. R. Kapral, Phys. Rev. 31A (1985) 3868.
[8] T. Yamada and H. Fujisaka, Prog. Theor. Phys. 72 (1985) 885.
[9] J. Crutchfield, private communication.
[10] J.D. Keeler and J.D. Farmer, Physica 23D (1986) 413.
[11] J. Crutchfield and K. Kaneko, in preparation (extensive review on spatio-temporal chaos).
[12] F. Kaspar and H.G. Schuster, Phys. Lett. 113A (1986) 451.
[13] R.J. Deissler, J. Stat. Phys. 40 (1985) 371; "Spatially Growing Waves, Intermittency, and Convective Chaos in an Open-Flow System" (submitted to Physica D, LA-UR-85-4211), and Ph.D. Thesis.
[14] R. Shaw, Z. für Naturforschung 36a (1983) 80.
[15] K. Matsumoto and I. Tsuda, preprint.
[16] The similar behavior has also been observed in the delay differential equation system (K. Ikeda and K. Matsumoto, private communication; see also J.D. Farmer, Physica 4D (1982) 366).
[17] P.W. Anderson, Phys. Rev. 109 (1958) 1492.
[18] S. Wolfram, Physica 10D (1984) 1; N. Packard, in Dynamical Systems and Cellular Automata (Academic Press, New York, 1985).
[19] B. Hasslacher, preprint (1985) (LA-UR-85-2435).
[20] K.R. Sreenivasan, in Frontiers of Fluid Mechanics, S.H. Davis and J.L. Lumley, eds. (Springer, New York, 1985) and private communication.
[21] F. Takens, in Dynamical Systems and Turbulence, D. Rand and L.S. Young, eds. (Springer, New York, 1981); N. Packard et al., Phys. Rev. Lett. 45 (1980) 712.
[22] For the case of a two-coupled system, see e.g., C. Froeschle, Astron. Astrophys. 22 (1973) 431; K. Kaneko and R. Bagley, Phys. Lett. 110A (1985) 435.